RL-TR-91-55
Final Technical Report
May 1991

ULTRA-HIGH FREQUENCY SUPERCONDUCTIVE DEVICES

Cornell University

Sponsored by
Strategic Defense Initiative Office

APPROVED FOR PUBLIC RELEASE; DISTRIBUTION UNLIMITED.

The views and conclusions contained in this document are those of the authors and should not be interpreted as necessarily representing the official policies, either expressed or implied, of the Strategic Defense Initiative Office or the U.S. Government.

Rome Laboratory
Air Force Systems Command
Griffiss Air Force Base, NY 13441-5700

This report has been reviewed by the Rome Laboratory Public Affairs Division (PA) and is releasable to the National Technical Information Service (NTIS). At NTIS it will be releasable to the general public, including foreign nations.

RL-TR-91-55 has been reviewed and is approved for publication.

APPROVED: John P. Turtle

JOHN P. TURTLE
Project Engineer

APPROVED: John K. Schindler

JOHN K. SCHINDLER
Director of Electromagnetics

FOR THE COMMANDER: Igor G. Plonisch

IGOR G. PLONISCH
Directorate of Plans & Programs

If your address has changed or if you wish to be removed from the Rome Laboratory mailing list, or if the addressee is no longer employed by your organization, please notify Rome Laboratory (EEAA) Hanscom AFB MA 01731-5000. This will assist us in maintaining a current mailing list.

Do not return copies of this report unless contractual obligations or notices on a specific document require that it be returned.

ULTRA-HIGH FREQUENCY SUPERCONDUCTIVE DEVICES

Robert A. Buhrman

Contractor: Cornell University
Contract Number: F19628-86-K-0034
Effective Date of Contract: 1 October 1986
Contract Expiration Date: 31 March 1990
Short Title of Work: Superconducting Mixers and Oscillators
Period of Work Covered: Oct 86 - Mar 90

Principal Investigator: Robert A. Buhrman
Phone: (607) 255-3732

RL Project Engineer: John P. Turtle
Phone: (617) 377-2051

Approved for public release; distribution unlimited.

This research was supported by the Strategic Defense Initiative Office of the Department of Defense and was monitored by John P. Turtle, RL (EEAA) Hanscom AFB MA 01731-5000 under Contract F19628-86-K-0034.

REPORT DOCUMENTATION PAGE

Form Approved OMB No. 0704-0188

1. AGENCY USE ONLY (Leave Blank)	2. REPORT DATE	3. REPORT TYPE AND DATES COVERED
	May 1991	Final Oct 86 - Mar 90

4. TITLE AND SUBTITLE
ULTRA-HIGH FREQUENCY SUPERCONDUCTIVE DEVICES

5. FUNDING NUMBERS
C - F19628-36-K-0034
PE - 63220C
PR - S812
TA - C1
WU - 22

6. AUTHOR(S)
Robert A. Buhrman

7. PERFORMING ORGANIZATION NAME(S) AND ADDRESS(ES)
Cornell University
School of Applied and Engineering Physics
Clark Hall
Ithaca NY 14853-2501

8. PERFORMING ORGANIZATION REPORT NUMBER

9. SPONSORING/MONITORING AGENCY NAME(S) AND ADDRESS(ES)
Strategic Defense Initiative Office, Office of the Secretary of Defense
Wash DC 20301-7100

Rome Laboratory (EEAA)
Hanscom AFB MA 01731-5000

10. SPONSORING/MONITORING AGENCY REPORT NUMBER
RL-TR-91-55

11. SUPPLEMENTARY NOTES
Rome Laboratory Project Engineer: John P. Turtle/EEAA/(617) 377-2051

12a. DISTRIBUTION/AVAILABILITY STATEMENT
Approved for public release; distribution unlimited.

12b. DISTRIBUTION CODE

13. ABSTRACT (Maximum 200 words)
The objective of this research program was to develop advanced superconducting tunnel junctions for application in superconducting local oscillators and mixers operating in the Terahertz (0.2 - 2.0 THz) frequency regime. The research was focused on the development of stable, all refractory, high-critical-current-density, small-area tunnel junctions based on NbN superconducting thin films. A successful process for the fabrication of rugged 1 μm^2 NbN-MgO-NbN Josephson tunnel junctions was developed with the junctions having critical current densities > 10^4 A/cm^2. The NbN tunnel junctions were found to be effective voltage-tunable Josephson oscillators from 300 GHz to above 1.4 THz. Direct measurement of the response of the detector junction indicated that the oscillator voltage was typically 1.5 mV in amplitude and thus the oscillator power was of the order of 0.5 µW in the THz regime. While clearly demonstrating the feasibility of producing practical Josephson junction oscillators and other Josephson devices for operation in the THz regime the experiment results also indicated that MgO tunnel barriers are less than a completely successful tunnel barrier material for NbN Josephson device applications.

14. SUBJECT TERMS
Superconducting, Josephson Junction, Oscillator, Tunnel Barrier, Terahertz

15. NUMBER OF PAGES 32

16. PRICE CODE

17. SECURITY CLASSIFICATION OF REPORT	18. SECURITY CLASSIFICATION OF THIS PAGE	19. SECURITY CLASSIFICATION OF ABSTRACT	20. LIMITATION OF ABSTRACT
UNCLASSIFIED	UNCLASSIFIED	UNCLASSIFIED	UL

INTRODUCTION

The objective of this research program was to develop advanced superconducting tunnel junctions for application in superconducting local oscillators and superconducting mixers operating in the Terahertz (0.2 - 2.0 THz) frequency regime. The research was focused on the development of stable, all refractory, high-critical-current-density, small-area tunnel junctions based on NbN superconducting thin films. A successful process for the fabrication of ~ 1 μm^2 NbN-MgO-NbN Josephson tunnel junctions was developed with the junctions having critical current densities > 10^4 A/cm^2. Such junctions were found to be very rugged and reliable. In experiments in which such junctions were coupled capacitively to a nearby, on-chip, Josephson junction detector, the NbN junctions were found to be effective voltage-tunable oscillators from 300 GHz to above 1.4 THz. Direct measurement of the response of the detector junction indicated that the oscillator voltage was typically 1.5 mV in amplitude. This indicated that the Terahertz oscillator power was of the order of 0.5 μW, of which, due to impedance mismatch, 0.01 μW was typically coupled into the detector junction. This power is quite adequate for local oscillator applications in Terahertz mixer applications that might employ a superconducting SIS detector. However, a narrowing of the oscillator linewidth by some means, such as through the use of a strip-line resonator, will be required for practical applications.

In addition to demonstrating the ultra-high frequency capability of high-critical-current density NbN junctions this research project also identified several problems, both process and materials related with the NbN-MgO-NbN tunnel junction system. These problems included device heating at the necessarily high critical current densities, difficulties in obtaining reproducible (i.e. repeatable critical current) junctions at the high critical current densities required and the excessive high level of 1/f noise found in the tunnel junction. The first problem was solved by careful device design. The latter two are more fundamental and strongly point to the conclusion that an alternative tunnel barrier material should be developed to replace the less than satisfactory MgO barrier in the NbN tunnel junction system.

DISCUSSION

This research project began with the objective of demonstrating the capability of Josephson junction local oscillators and detectors for successful device operation in the ultra-high, Terahertz, frequency regime, 0.3 to 3.0 THz. To operate successfully at very high frequencies a Josephson tunnel junction must have sufficiently high conductance per unit area such that the junction resistance is comparable to, or less than, the junction's shunt capacitance. Since the conductance per unit area of a Josephson tunnel junction is directly proportional to its superconducting critical current density J_c, the above condition is equivalent to requiring that for frequencies above 200 GHz, we must have $J_c \sim 10^4 - 10^5$ A/cm^2. In general it has proven difficult to reliably produce tunnel junctions with sufficiently thin tunnel barriers to yield this range of values of J_c. Moreover when such junctions were produced the quality of the resultant I-V characteristic was such that there were serious questions about the nature of the Josephson currents at high bias voltages which approach the gap-sum voltage, which by the ac Josephson relation is equivalent to very high frequencies.

Accordingly, we began our research effort by examining the behavior of Josephson devices that were fabricated in an unique double-edge-junction structure. This structure readily permitted the fabrication of pairs of very high critical-current-density Josephson junctions with comparably good I-V characteristics and with a design that optimized cooling of the active device area by facilitating rapid diffusion of quasiparticles from the active device area. Using one junction as a voltage-tunable Josephson oscillator and the other as a Josephson detector these devices permitted direct measurement of the oscillating Josephson pair current from bias voltages (oscillating frequencies) ranging from 1.20 mV (600 GHz) to 1.8 mV (900 GHz). The Josephson junctions used in this measurements employed Nb and Sn electrodes and accordingly this voltage range extended from well below the gap sum region up to and slightly past the gap-sum voltage. These preliminary results directly demonstrated that large ac Josephson currents are certainly obtained in the ultra-high frequency regime, even if the tunnel junction characteristic is less than ideal.

Following this initial feasibility demonstration, our attention turned to developing an NbN thin film and small area, high J_c tunnel junction technology and then to implementing this technology in the fabrication and testing of a $NbN_{1-x}C_x$ Terahertz oscillator chip. A successful process for reactively sputter depositing rather high quality $NbN_{1-x}C_x$ (NbN for short) thin films at or near room temperature was developed. This room temperature deposition process was required in order to be compatible with the entire fabrication procedure for the Terahertz oscillator chip, a procedure that ultimately involved a considerable number of separate deposition and lithography steps. A trilayer NbN - MgO - NbN deposition process was then developed, which when combined with a high resolution photolithography and reactive etching procedure resulted in the formation of small area (~ 2μm^2) high critical current density ($J_c > 10^4$ A/cm^2) tunnel junctions with acceptable, if not ideal I-V characteristics. The successful development of this challenging junction fabrication process was a major milestone in the research program.

With the satisfactory development of a NbN - MgO - NbN junction technology, the research effort then focused on the design and fabrication of a Terahertz oscillator test chip. This chip consisted of NbN Josephson junction oscillators capacitively coupled to small area (0.1 μm^2) Josephson junction detectors. In order to separate out the frequency response of the detector from that of the oscillator junction, the detector was chosen to be a Nb - Nb_2O_5- Sn edge junction. The design of the device structure was carefully optimized to minimize local heating of the Josephson oscillator and detector junctions and to maximize coupling of the Josephson oscillator voltage to the detector junction. The total Terahertz Chip fabrication process involved more than 10 thin film layers and numerous fabrication steps. After considerable efforts complete chips were successfully fabricated and extensively tested.

The Josephson junction oscillator tests were rather successful. The NbN tunnel junctions typically had $J_c \sim 4 \times 10^4$ A/cm^2 and were directly measured with the detector junction to produce an oscillating junction voltage of ~ 1.5 mV. The detected rf voltage level was found to remain essentially constant from 300 GHz to above 1 THz. Typically the oscillator was found to produce approximately 0.5 μW of Terahertz radiation of which, due to impedance mismatch, 0.01 μW was coupled into the detector junction. This power level is more than adequate for the purposes of a local oscillator in a Terahertz receiver application. Of course now that the feasibility of a NbN based Terahertz oscillator has been experimentally established, the extension of this device to a resonantly coupled stripline array of such junctions to increase the output power and narrow the oscillator linewidth, as has been done with Nb junctions at lower frequencies, appears to rather straightforward.

One aspect of the oscillator junction results that was a bit surprising was the finding that the ac supercurrent response of the Josephson junctions at voltages (frequencies) above the gap-sum voltage (frequency) did not follow the predictions of the widely accepted Werthamer theory of the Josephson effect. Instead the ac supercurrent amplitude was found to decrease much more rapidly as the oscillating frequency was increased above the gap-sum frequency than predicted theoretically.

This measurement is actually in accord with much earlier, previously unexplained, results on the ac response of Josephson junctions that were obtained in a different and less direct measurement. Thus this rapid decrease in ac supercurrent amplitude may be rather general, but it has not yet been established whether the disagreement is due to a fundamental problem with the theory or to less than ideal behavior in real tunnel junctions. We are continuing to search for a successful explanation for this observation and note that it does appear to limit the useful range of Josephson junction oscillators to frequencies not much greater than the gap sum frequency. Since for the best quality NbN junctions this upper limit is approximately at 2.5 THz, this does not currently appear to be a very restrictive limit.

Following our successful demonstration of the Terahertz oscillator chip, attention then turned to the fabrication of a second generation, all NbN junction chip that would have permitted tests of the Josephson oscillator to still higher frequencies as well as tests of several very simple two-junction coupled oscillator designs. Unfortunately equipment problems and the difficulties of maintaining a reliable MgO tunnel barrier process prevented this effort from being successfully completed before the end of the funding period.

This final effort did have the effect of concentrating our attention onto the properties of the MgO tunnel barrier. From a variety of analytical and tunnel junction studies of these barriers it seems quite clear now that the choice of an MgO barrier for NbN tunnel junctions leaves quite a bit to be desired. Both in our experiments and in experiments performed elsewhere it is a general fact that the best results that have been obtained with deposited MgO layers is considerably below that which has been obtained with, for example, Nb_2O_5 barriers formed by thermally oxidizing the NbN base layer. Of course Nb_2O_5 cannot be used with a NbN counterelectrode due to its instability during NbN (or Nb) condensation. The NbN - MgO - NbN junctions are also quite inferior with regard to reproducibility and quality when compared to the almost universally used Nb-(Al)- Al_2O_3 - Nb junction technology. While MgO barriers were originally introduced with the NbN system because of the fairly close lattice match between NbN and MgO the problem appears to be that this lattice match does not remove the very strong effect on junction properties caused by the high level of stress that is found in sputter deposited NbN films. It appears that this stress, on an atomic scale, results in structural instabilities in the MgO layer which in turn results in the formation of leakage paths through the barrier and in a considerable variation in barrier resistances for nominally identical junctions. The existence of these instabilities is directly seen in the extremely high values of excess low frequency or 1/f noise that is found in these junctions, both those fabricated at Cornell and in several that we tested that were supplied by Dr. Brian Hunt of JPL. In a separate experimental program we had previously determined that 1/f noise in tunnel junctions arises from atomic scale fluctuations of structural defects in the tunnel barrier. Thus the fact that these MgO barriers exhibit 1/f noise levels that are typically two orders of magnitude greater than that generally seen in the better quality Nb_2O_5 and Al_2O_3 tunnel barriers is a clear signal of fairly fundamental problems with the NbN - MgO - NbN tunnel junction technology.

CONCLUSIONS

This research project was intended to examine the nature of the ac Josephson effect in the Terahertz frequency regime and to develop a high critical current density, small area, all NbN junction technology that would be suitable for local oscillator and perhaps for Josephson mixer applications in the Terahertz regime. We have fabricated such junctions and have successfully demonstrated Josephson oscillator performance in the frequency regime extending from 300 GHz to above 1.5

THz. The results are more than sufficient to show that practical realizations of Josephson devices in this frequency regime can be readily achieved. While departures from the accepted Josephson theory at frequencies above the gap-sum frequency were clearly observed, the power level and overall behavior of the Josephson oscillator below the gap-sum frequency is in quite reasonable accord with expectations. Extensions of the oscillator results to the case of coupled junction arrays should be expected to result in practicable oscillators for Terahertz receiver systems. Materials problems arising from the choice of MgO for the tunnel barrier were identified and attributed to structural instabilities in the tunnel barrier, most probably caused by the high levels of stress in the various thin film materials comprising the tunnel junction. A important conclusion to be drawn from this work is that MgO does not appear to be a fully satisfactory answer to the need for a tunnel barrier material that is compatible with an all NbN junction technology. The most important step that could be taken to significantly advance the feasibility of Josephson junction applications based on NbN thin films would be to undertake a focused effort to develop an improved tunnel barrier material as a successful substitute for MgO.

PUBLICATIONS

More complete details of results arising from this research program can be found in the technical publications that are appended to this report. A very complete report can be found in the Ph. D. thesis of Dr. R. P. Robertazzi, Cornell University, Ithaca, NY (1990), unpublished. Copies of this thesis can be obtained from the Principal Investigator upon request.

JOSEPHSON TERAHERTZ LOCAL OSCILLATOR

R. P. Robertazzi, R. A. Buhrman
School of Applied and Engineering Physics
Cornell University
Ithaca, New York 14853-2501

Abstract

Voltage tunable Josephson junction Terahertz oscilla-rs have been fabricated using rugged, high current density bN$_{1-x}$C$_x$ tunnel junctions with MgO barriers. The radia-on emitted from such junctions is detected on chip by a sec-nd Josephson junction which is capacitively coupled to the rst. For oscillator junctions with a critical current density of $_c \sim 3.5 \times 10^4 A/cm^2$ we find that the junction oscillates with a oltage amplitude of $\sim$ 1.5 mV. The detected RF voltage level emains essentially constant from 300 GHz. to above 1 THz, he upper limit of the detector. From measurements of the osephson step height in the detector IV it is determined that he oscillator junction is producing 0.5 μW of Terahertz radi-tion of which, due to impedance mismatch, 10 nW is coupled nto the detector junction.

Introduction

The production and detection of sub-millimeter wave sig-als for communications systems and radio astronomy applica-ions presents severe engineering problems for even state of the rt compound semiconductor (GaAs) devices. For this reason here has been much interest in the application of Josephson unctions as high frequency, voltage tunable oscillators. Al-hough the power available from a single device is low the use f these devices in a coupled array configuration could signifi-antly boost the available power [1]. The focus of our research rogram has been the development of a device in which a high urrent density NbN$_{1-x}$C$_x$/MgO/NbN$_{1-x}$C$_x$ tunnel junction capacitively coupled to an SIS detector junction to measure he high frequency response of these junctions when biased to erve as local oscillators. Our results indicate that NbN$_{1-x}$C$_x$ unctions can be successfully employed as local oscillators at requencies well above 1 THz.

Device Fabrication

In figure 1 is shown a schematic representation for the ntegrated thin film microstructure used in this experiment. It onsists of two SIS devices coupled at RF frequencies but DC olated so that each may be individually biased. One junction a trilayer mesa type [2] formed with NbN$_{1-x}$C$_x$ base and ounter electrodes and an MgO barrier. The second junction is an edge type [3] utilizing a Nb base electrode with a native oxide Nb$_2$O$_5$ barrier and Sn counter electrode. In normal operation the mesa junction is biased to serve as the local oscillator and the edge junction serves as a Josephson RF detector. A Nb-Sn detector junction was used in this experiment to permit the study of the response of a Josephson junction at frequencies well in excess of the gap sum frequency.

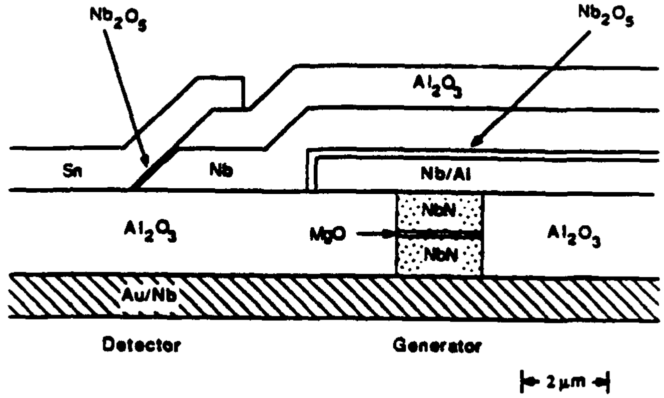

Figure 1: Integrated thin film microstructure used in the local oscillator experiments. The bimetallic layers are shown as single layers for clarity. Vertical scales are greatly exaggerated.

The fabrication process starts with unoriented sapphire substrates onto which a bimetallic Nb/Au wiring is deposited using standard photolithographic lift-off techniques. Onto these substrates a NbN$_{1-x}$C$_x$/MgO/NbN$_{1-x}$C$_x$ trilayer is sputtered without breaking vacuum. NbN$_{1-x}$C$_x$ is reactively sputtered from a Nb target in an Ar/N$_2$/CH$_4$ ambient [4,5] with no intentional substrate heating. The films are characterized by a high transition temperature (T_c = 15.5 K) and sharp transition width ($\Delta T \sim 0.1$ K). To obtain this result we find that very close control of the sputter gas ambient pressure and composition are required. MgO barriers are RF sputtered in a 10 millitorr Ar ambient.

After the trilayer deposition the films are chemically etched to remove most of the trilayer except for areas 30 μm square over the active device area. The final 2 μm × 2 μm junctions are defined by reactive ion etching of the larger 30 μm squares using photo resist as a mask. The etch mask also serves as a lift-off stencil for the insulation of the sides and base electrode of the junction in a self aligning process very

Manuscript received August 22, 1988.

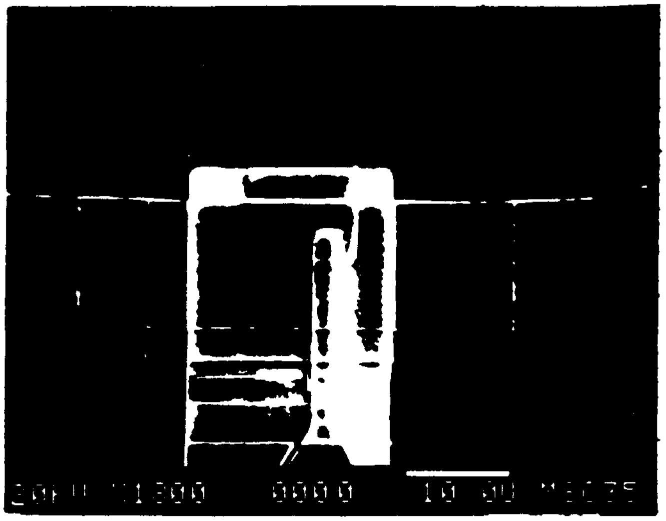

Figure 2: Scanning electron micrograph of generator - detector device.

similar to the one developed by Shoji et. al.[2] After reactive ion etching in a 20% O_2/CF_4 plasma Al_2O_3 is electron beam evaporated and lifted off. Al_2O_3 is used as a insulator because its low dielectric constant ($\epsilon_{Al_2O_3} = 5$) [6] keeps parasitic loading of the oscillator to a minimum. After insulation, lift-off stencils are applied for wiring patterns to contact the counter electrode. The counter electrode is etched with an ion mill, followed immediately by the deposition of Al (2000 Å) and Nb (400 Å). The Al provides a low strain, high thermal conductivity path away from the junction which along with the Au base electrode wiring helps to minimize self heating of the oscillator under bias, an important feature of this design in light of the requirement of high current density and the relatively low thermal conductivity of $NbN_{1-x}C_x$. Once the oscillator contact process is complete the Nb layer is chemically anodized [7] to grow 350 Å of Nb_2O_5, ($\epsilon_{Nb_2O_5} = 29$) [8]. This insulating layer forms the dielectric of the coupling capacitor. Over this 1500 Å of Nb is sputtered, followed by 2000 Å of Al_2O_3. This last layer forms the base electrode for the detector junction. An inert ion beam is used to etch the edge of this thin film stack, after which a counter electrode stencil is applied, through which the tunnel barrier is formed by reactive ion beam oxidation [3]. The counter electrode is deposited and lifted off. An SEM photo of the completed device is shown in figure 2. Of course through use of $NbN_{1-x}C_x$ for the base and counter electrodes the minimum operating temperature of the integrated oscillator - detector microstructure could be raised to 10 K. A typical current - voltage (IV) curve of a high current density generator is shown in figure 3a. The gap sum of the detector (1.8 mV) is somewhat reduced from the full theoretical value (2 mV) because of impurities in the Nb film. The generator gap sum is reduced from 5 mV to 4 mV because the $NbN_{1-x}C_x$ is off stoichiometry. Figure 3b shows the IV characteristic of the detector junction taken with the generator junction unbiased.

Equivalent Circuit

The edge junction base electrode together with the common Au wiring forms a transmission line which is capacitively coupled to the generator. The typical generator operating frequency is 1 THz. At this frequency the signal wavelength is,

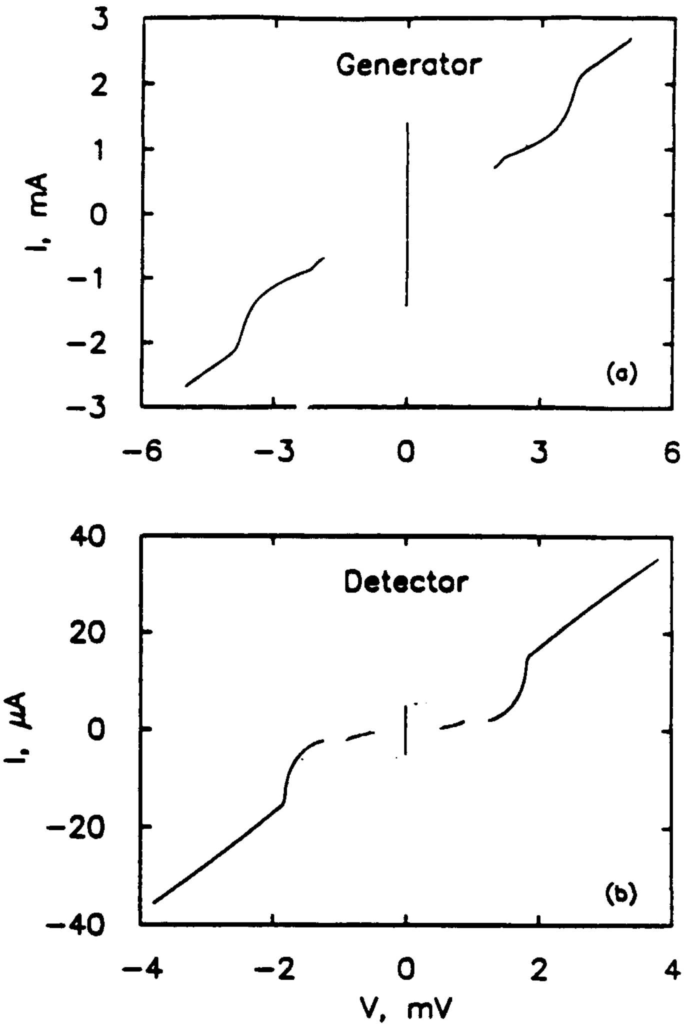

Figure 3: (a) IV characteristic of generator, $J_c = 3.5 \times 10^4 A/cm^2$, $R_n = 1.9\Omega$. (b) IV characteristic of detector. $J_c = 2.3 \times 10^3 A/cm^2$, $R_n = 110\Omega$.

$\lambda = 130\mu m$ (correcting for the dielectric constant of Al_2O_3). which is much longer than the 10 μm length of line between the generator and detector. Consequently we may approximate the phase of the signal as being constant over the length of the coupling structure and use a simple AC circuit to model the device. The equivalent circuit is shown in figure 4. C_c represents the coupling capacitor, L_p and C_p the parasitic inductance and capacitance respectively associated with the coupling structure. For the dimensions shown in figure 1 we have C_c= 0.7 pf, L_p = .24 ph, and C_p = 0.05 pf. This means that at an oscillator frequency of 2 THz., for oscillator impedances of $\sim 1\Omega$, detector impedances of $\sim 20\Omega$ or greater, the coupling efficiency $\eta = V_d/V_g$, where V_d is the amplitude of the detected signal and V_g is the amplitude of the oscillator signal at the generator approaches unity. For the device whose IV characteristics are shown, taking the normal state resistances of the junctions. $R_g = 1.9\Omega$, $R_d = 110\Omega$, and $\eta \sim 1$. In this design η remains close to unity even for frequencies down to 100 GHz., which represents a range of over a factor of 20 in frequency over which the coupling efficiency is essentially unity.

When DC biased, the generator will produce an oscillating

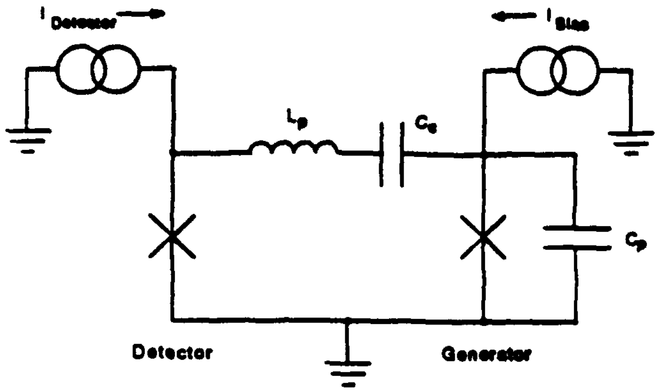

Figure 4: Equivalent circuit model of the double tunnel junction device.

voltage signal V_g at a frequency determined by the Josephson relation

$$f = 2eV_{bias}/h. \tag{1}$$

Here V_{bias} is the average voltage across the junction. V_g will be determined by the total capacitive loading of the generator. When the McCumber parameter β_c defined by [9]

$$\beta_c = (2e/\hbar)(I_cR_n)(R_nC) \tag{2}$$

is less than unity the junction is not capacitively shunted and the maximum V_g obtainable is approximately I_cR_g, at least for $V_{bias} < 2\Delta$.

At T = 0 the I_cR_n product is related to Δ through the Ambegaokar-Baratoff [10] relation

$$I_cR_n = \frac{\pi}{2}\frac{\Delta}{e}. \tag{3}$$

Thus larger oscillator signal amplitudes, as well as higher frequencies, are possible with higher Δ materials. This is part of the motivation in the choice of $NbN_{1-x}C_x$ for the generator base and counter electrodes. The capacitance in expression (2) is the total capacitance seen by the generator at the oscillation frequency which by design of the coupling structure is dominated by the junction capacitance. For a deposited MgO barrier 10 Å thick this capacitance is C = 0.3 pf assuming $\epsilon_{MgO} = 9.7$ [2]. This gives $\beta_c(gen) = 6$ so the generator is partially shunted and its IV characteristic is hysteretic. The degree of hysteresis shown in figure 3a is consistent with numerical estimates.

Oscillator Performance

When the generator is DC biased and if it emits radiation of sufficient power constant voltage steps will be induced in the IV of the detector at integral multiples of V_{bias} [11]. Figure 5 shows the detector characteristic with the generator biased at 1.090 mV. The N = 1 and N = 2 steps are clearly visible, as well as the depression of the supercurrent (N = 0 step). The detector sees at RF frequencies a low impedance generator, consequently it is appropriate to model the detector as being driven by an RF voltage source. According to the voltage biased theory [12] the size of the Nth induced step is given by

$$\Delta I_N = I_c\left|J_N(\alpha)\right|. \tag{4}$$

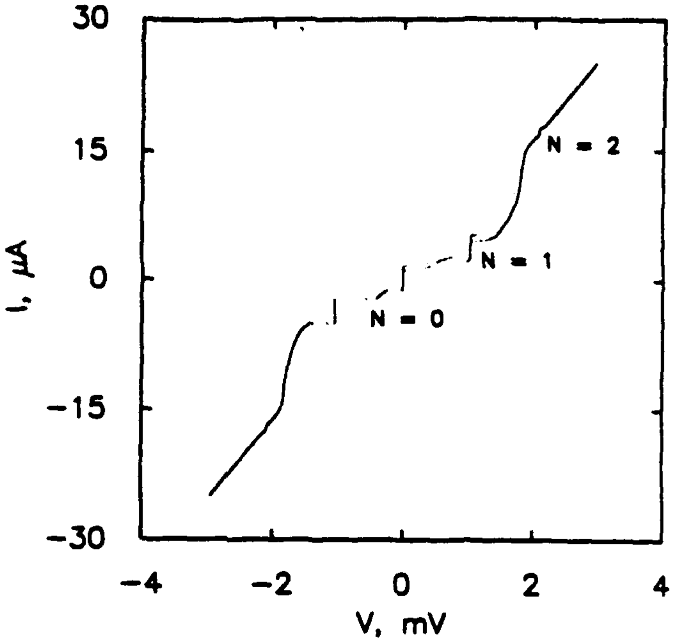

Figure 5: IV characteristic of detector junction with generator biased at $V_{bias} = 1.090$ mV. The N = 1 and N = 2 Josephson steps are marked, as is the supercurrent (N = 0).

Here $\alpha = 2eV_d/hf = V_d/V_{bias}$, and $J_N(x)$ is the Bessel function of the first kind of order N. For the steps on the detector IV in figure 5 both the generator and detector critical currents were suppressed by a magnetic field used to allow biasing the generator at this low frequency. The detected power is thus reduced. By taking the ratio of the current widths of the N = 0 and N = 1 steps and using equation (4) we may solve for α. This is more accurate than applying equation (4) directly since flux trapping makes the precise determination of I_c difficult.

Assuming a coupling efficiency of unity we find $V_g = 1.54$ mV, 58 % of the maximum value of 2.66 mV set by the I_cR product in the low β_c limit. While according to equation (2) to achieve the $\beta_c \sim 1$ limit a critical current density of $J_c = 3 \times 10^5 A/cm^2$ is required we find that with a hysteretic IV characteristic and a generator critical current density of $J_c = 3.5 \times 10^4 A/cm^2$ an RF power of 12 nW is being coupled into the 110Ω detector junction. This corresponds to a peak generator power of $V_g{}^2/2R_g = 0.6\,\mu W$ which is poorly coupled into the detector because of the large impedance mismatch (50 : 1) of the detector and generator. Thus we find that single, unshunted tunnel junctions can emit a comparably high level of submillimeter wave radiation even when the critical current density $J_c \sim 10^4 A/cm^2$ is such that the junction is partially hysteretic and $\beta_c > 1$.

Generator Self Heating

In designing the biasing structure the self heating of the generator junction under bias and the local rise in temperature at the detector are important considerations. A measurement of the effectiveness of the biasing structure as a heat sink can be obtained by comparing the IV characteristic of the generator with the sample cell filled with He gas and then filled with He liquid to improve thermal contact to the bath. We have observed negligible changes in the gap sum voltage under these two conditions and conclude that self suppression effects of the generator are small at these current densities, assuming that, as is generally the case, heat transport away from the junction is substantially increased by the presence of liquid He. Another means of examining device heating is to monitor the local temperature at the detector by measuring the Sn gap as a function of power dissipation of the generator. At a bath temperature of 1.5 K, we find that biasing the generator at 24 μW will raise the temperature of the detector, which is only 12 μm from the generator, 2.2 K when only He exchange gas is present in the sample cell. With liquid He in the cell more than 5.5 times more power is required to produce the same temperature rise. When biased at the gap edge the generator dissipates 7.5 μW, so with liquid introduced into the cell adequate heat sinking should be obtainable with generator current densities well into the $10^5 A/cm^2$ range. Of course it is possible that if the heating is more localized self heating of the oscillator could begin to be a problem in this higher current density range. Since our experiments demonstrate that $J_c \sim 5 \times 10^4 A/cm^2$ is adequate for Terahertz operation this should not be a concern. Using an all $NbN_{1-x}C_x$ detector junction would further reduce the effects of small temperature rises on detector performance.

High Frequency Pair Current Response

We have measured the frequency dependence of the pair current response as the generator bias is tuned through the gap sum of the detector. At frequencies approaching and in excess of the gap-sum the expression (4) is no longer valid and the full high frequency theory which takes into account the frequency dependence of the pair current must be used [13]. With the application of the frequency dependent theory we find good general agreement with experiment up to the gap sum frequency but above this frequency the the Josephson response decays much more rapidly than is predicted by the theory. These results are consistent with previous measurements we have made on even more closely coupled tunnel junctions [14]. Our results do indicate that the generator with its higher gap sum is functioning at frequencies at least up to 1.4 THz. Experiments with a higher gap sum detector junction are now in progress to examine this ultra high frequency limit in more detail.

Conclusions

In conclusion, we have designed, developed, and fabricated an integrated thin film microstructure for the study of the performance of high current density, unshunted Josephson tunnel junctions as high frequency local oscillators. The local oscillator is directly coupled to the detector by an RF capacitor, to achieve highly efficient broad band coupling. We have succeeded in coupling nearly 60% of the maximum LO voltage signal available into an SIS detector junction over a frequency range from 300 GHz. to 1.0 above THz. The incorporation of an all refractory detector junction into the device would raise the minimum operating temperature to 10 K, in the range of closed cycle He refrigerators. Furthermore, there is a possibility of modifying this device for Teraherts heterodyne mixing applications.

Acknowledgements

This work was sponsored by Air Force contract F19628-86-K-0034 with RADC, funded by SDIO/IST and by the National Science Foundation through use of the facilities of the National Nanofabrication Facility and of the Cornell Materials Science Center.

References

[1] J. E. Sauvageau, A. K. Jain, J. E. Lukens, IEEE Trans. Magn., Mag-23, page 1048, 1987.

[2] Akira Shoji, Masahiro Aoyagi, Shin Kosaka, Fujitoshi Shinoki, Hisao Hayakawa, Appl. Phys. Lett., 46, page 1098, 1985.

[3] A. W. Kleinsasser, R. A. Buhrman, Appl. Phys. Lett., 37, page 841, 1980.

[4] S. A. Wolf, D. U. Gubser, T. L. Francavilla, E. F. Skelton. J. Vac. Sci. Technol., 18, page 253, 1981.

[5] H. D. Hallen, Private Communication.

[6] B. W. Davis, Infrared Physics, 22, page 91, 1982. Value of $\epsilon_{Al_2O_3}$ extrapolated from low frequency IR transmission data on sapphire.

[7] R. E. Joynson, C. A. Neugebauer, J. R. Rairden, J. Vac. Sci. Technol., 4, page 171, 1967.

[8] S. Basavaiah, J. H. Greiner, J. Appl. Phys., 47, page 4201. 1976.

[9] D. E. McCumber, J. Appl. Phys., 39, page 3113, 1968.

[10] V. Ambegaokar, A. Baratoff, Phys. Rev. Lett. 10, page 486, 1963.

[11] S. Shapiro, Phys. Rev. Lett., 11, page 80, 1963.

[12] S. Shapiro, A. R. Janus, S. Holly, Rev. Mod. Phys., 36, page 223, 1964.

[13] N. R. Werthamer, Phys. Rev., 147, page 255, 1966.

[14] R. P. Robertazzi, B. D. Hunt, R. A. Buhrman, IEEE Trans. Magn., Mag-23, page 1271, 1987.

COUPLED JOSEPHSON LOCAL OSCILLATOR AND DETECTOR EXPERIMENTS IN THE TERAHERTZ REGIME

R. P. Robertazzi, H. D. Hallen, and R. A. Buhrman
School of Applied and Engineering Physics
Cornell University
Ithaca, NY 14853-2501

1. Abstract

Recent coupled Josephson junction experiments in our laboratory have demonstrated that high critical current density tunnel junctions can serve as effective local oscillators at frequencies up to and in excess of the gap sum frequency of the junction, i.e. well above 1 Terahertz for a niobium or niobium compound tunnel junction. While the details of the behavior of such a THz. oscillator were found not to be in accord with the predictions of the accepted theory of the A.C. Josephson effect in the gap region significant radiation could be capacitively coupled from the oscillator junction to an adjacent junction, sufficient for SIS mixer experiments at Terahertz frequencies. Research efforts are now under way to further extend and expand these studies. A high critical current density all NbN tunnel junction system is now under development for Terahertz applications and a new set of coupled Josephson oscillator - SIS detector experiments is being initiated using NbN tunnel junctions. In this paper we will review the original coupled junction high frequency experiments and report on the recent progress of the current NbN tunnel junction experiments.

2. Introduction

The production and detection of sub-millimeter wave signals for communications systems and radio astronomy applications presents severe engineering problems for even state of the art compound semiconductor (GaAs) devices. SIS tunnel junctions used as mixers have been demonstrated to show superior performance over semiconductor (Super Schottky) mixer elements for frequencies less than 100 GHz. Theoretical predictions indicate that quantum limited detection sensitivity is possible in high quality SIS devices at these and higher frequencies. Our research program has focussed on several goals. We have investigated the high frequency pair current response of a Josephson tunnel junction for use as a local oscillator for heterodyne detection of THz. signals. These experiments will be described in the next section. Currently, we are also developing all refractory, high current density Josephson tunnel junctions for local oscillator experiments at higher frequencies. Refractory junctions are desirable because their durability allows them to survive post junction fabrication processing so they may be incorporated into practical, very high frequency detection circuits.

3. Previous Experiments

Our previous work involved the fabrication of a device which consisted of two high current density capacitively coupled tunnel junctions shown in figure 1. The device consists of two junctions formed on the edges of a thin film stack [1]. The capacitive coupling arises through the thin 500Å layer of Al_2O_3 separating the base Nb electrodes. Reactive ion beam oxidation was used to form the tunnel barrier, over which the counter electrode was deposited (Sn in this case). The equivalent circuit model of this device is shown in figure 2.

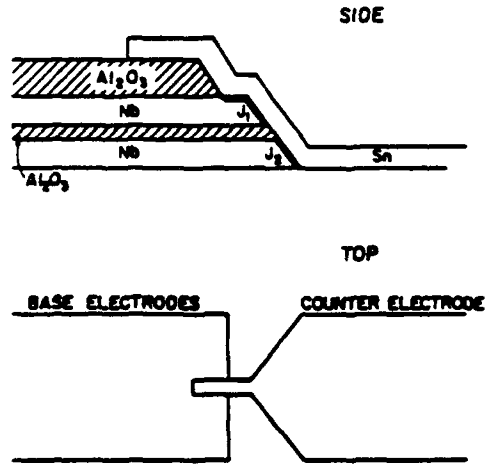

Figure 1. Double coupled tunnel junction device in cross section and from top view.

For a Josephson tunnel junction to serve as an effective local oscillator (LO) its capacitive shunt impedance must be higher than its normal state impedance R_n at the desired LO frequency, and its dynamic impedance at the bias point should be as low as possible for a narrow oscillator line width. This necessitates the fabrication of high current density junctions or alternatively resistively shunting the junction which reduces the LO power and leads to the requirement of fabricating junction arrays. For LO's the McCumber parameter β_c, defined by

$$\beta_c = (2e/\hbar)(I_c R_n)(R_n C) \tag{1}$$

is constrained to be less than 1. Here I_c is the critical current, and C is the junction capacitance. By biasing the the device with a constant D.C. current an average D.C. voltage V_{bias} will develop across the junction. In accord with the A.C. Josephson effect, an A.C. voltage will develop across the junction, the frequency of the oscillation being determined by the Josephson relation

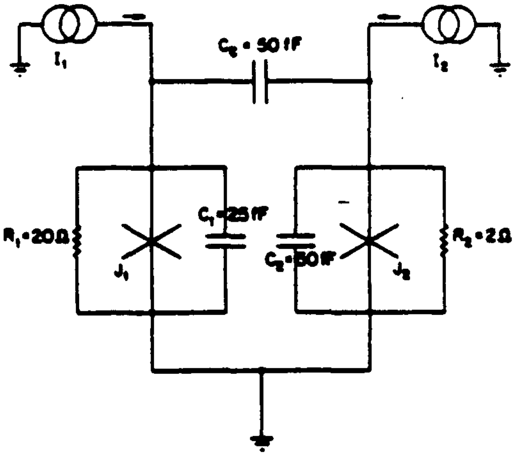

Figure 2. Equivalent circuit schematic for the double tunnel junction device.

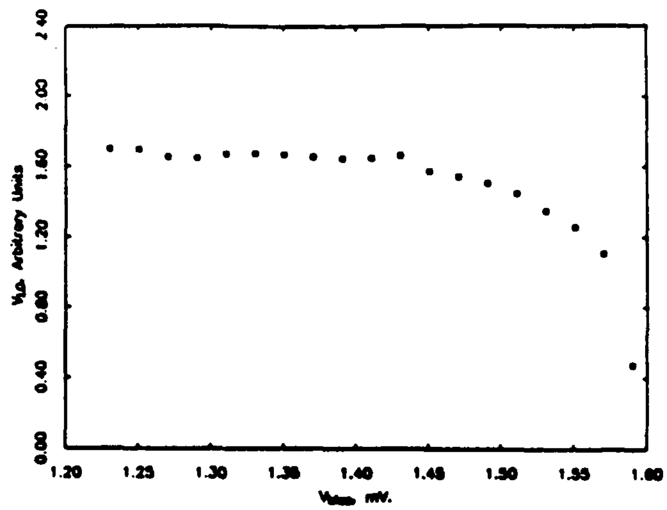

Figure 3. Measured local oscillator signal strength V_{LO} vs. V_{bias}.

$$\omega = 2eV_{bias}/\hbar. \tag{2}$$

The junction biased in this manner is a voltage controlled oscillator where the voltage to frequency conversion is $2e/h = 0.484THz./mV$.

We have measured the LO power output as a function of frequency using our double tunnel junction device. As a consequence of the A.C. Josephson effect, an A.C. signal coupled into a junction will be mixed down to D.C. and appear as a constant voltage current step in the current - voltage (IV) characteristic. The size of the step can be related to the oscillator power coupled into the device. Referring to figure 2, in our experiment J_2 was biased to serve as the LO and J_1 was used as the detector. The measured power output of J_2 as a function of frequency is shown in figure 3. For this particular set of junctions 12.5 nW was coupled into J_1 at 0.73 THz.

The theoretical frequency dependence of LO power for low β_c junctions for frequencies approaching the gap sum frequency is complex and not in agreement with our measurements for frequencies in excess of the gap sum, $V_{bias} > \Delta_1 + \Delta_2$. A more precision measurement of the frequency dependence of LO power in this region will be the focus of future experiments. However, for frequencies less than or equal to the gap sum frequency our experimental results do agree reasonably well with calculations based on the high frequency pair current theory. In this frequency regime both experiment and calculation verify that the maximum signal amplitude of the LO is well approximated by the I_cR_n product, i.e.

$$V_{LO} \sim I_cR_n \qquad (\beta_c \leq 1). \tag{3}$$

For an ideal Josephson junction this value is related to the energy gap

$$I_cR_n = \frac{\pi}{2}\frac{\Delta}{e}. \tag{4}$$

Eqn. (4) implies that LO power may be increased by using large Δ materials, in addition to raising the maximum operating frequency of the device, $\hbar\omega_{max} = 4\Delta$.

4. Current Research

Our current research program in NbN films for use in high current density Josephson tunnel junctions was motivated by the desire to achieve higher operating frequencies and LO power outputs, as well by practicality. Edge junction devices with soft counter electrodes and native oxide barriers are excellent research tools but lack the ruggedness to survive post junction fabrication processing needed to incorporate the devices into useful circuits, i.e. real world electronics. Furthermore, the fabrication of Josephson junctions with high T_c electrodes ($T_c \sim 16°K$) would allow operation at $10°K$, within the limits of closed cycle refrigerators.

Our NbN films are produced by the reactive sputtering of Nb in an atmosphere of Ar, N_2, and CH_4. The films are sputtered with no intentional substrate heating at a rate of approximately $40Å/sec$. Films produced in this way are smooth and have high transition temperatures. Figure 4 shows a resistance v.s. temperature plot of a typical NbN film. The film has a transition temperature $T_c = 15.5K$, a transition temperature width $\Delta T_c = 0.1K$ and a residual resistance ratio $RRR = 0.96$. The narrow transition temperature width is important for the fabrication of high quality junctions with small dynamic resistance at the gap edge because a distribution in transition temperatures implies a distribution in the superconducting energy gap. If this smearing in Δ is present in the tunnel junction near the barrier the sharpness of the IV curve at the gap edge will be reduced. Since it is desirable, both for mixing and LO signal production, to keep the rise in current at the gap edge as sharp as possible highly uniform films are desirable.

In our all refractory junction process MgO is sputtered to form the artificial tunnel barrier. Our process is quite similar to others developed previously. A NbN/MgO/NbN trilayer is

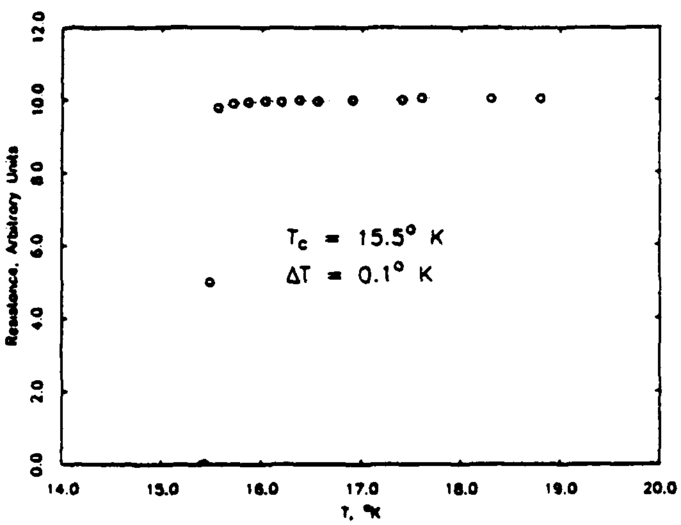

Figure 4. Resistance vs. temperature for a typical NbN film.

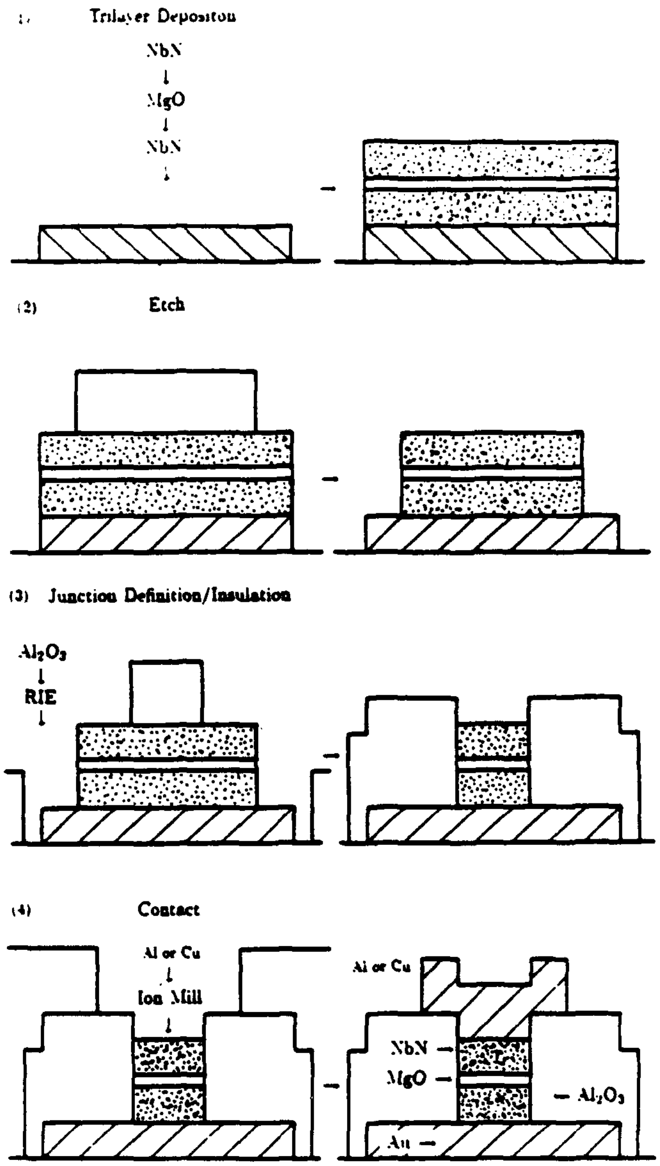

Figure 5. Fabrication process for all refractory NbN/MgO/NbN Josephson tunnel junctions.

sputtered, without breaking vacuum over a sapphire wafer with Au contact pads previously deposited. The trilayer is etched, first with a wet etch and then with RIE to define the $2\mu \times 2\mu$ junctions. Al_2O_3 is used to insulate the junction sides and base electrode wiring. Further photolithography defines the counter electrode wiring, which is typically Cu or Al to aid in the removal of heat from the junction while the junction is biased. The entire process is shown schematically in figure 5.

Some typical junction characteristics are shown in figure 6. Figure 6a shows the IV characteristic of a junction with a critical current density $J_c = 5 \times 10^3 A/cm^2$, $V_m = 12mV.$, and $2\Delta = 4.1mV$. Figure 6b shows the IV of a higher current density junction, $J_c = 4 \times 10^4 A/cm^2$, $V_m = 4mV.$, and $2\Delta = 4mV$. Future process work will concentrate on raising 2Δ, V_m, and J_c. We have subjected these devices to post junction fabrication photolithographic processing as well as thermal cycling between 300 K and 4.2 K, and have found them to be quite durable.

Our ultimate goal is to produce high quality junctions with a critical current density of $5 \times 10^5 A/cm^2$ so $\beta_c \leq 1$. Of course in such high current density junctions non-equilibrium and local heating problems will likely be a serious concern. But previous experiments in our laboratory with small area, high current density tunnel junctions have shown that such effects can be alleviated through the use of efficient fan-out geometries that permit the rapid diffusion of non-equilibrium quasiparticles from the active junction area.

Our initial experimental goal is to use these high current density junctions to make more precise and unambiguous measurements of the pair current response of a Josephson tunnel junction at frequencies close to and greater than the gap sum. We propose to establish the suitability of such junctions for use as LO's for heterodyne mixing of THz. signals. The line width of a Josephson junction oscillator biased at a D.C. voltage V_0 has the theoretical form [2]:

$$\Delta\omega = \left(\frac{2e}{\hbar}\right)^2 R_d^2 \Big[2eI_{Pair}(V_0)coth(\beta eV_0) + eI_{Qp}(V_0)coth(\beta eV_0/2) + 2eI_{Qp-Pair}(V_0)coth(\beta eV_0)\Big] \quad (5)$$

Here I_{Pair}, I_{Qp}, and $I_{Qp-Pair}$ are the pair, quasiparticle and quasiparticle - pair interference currents at a voltage V_0 respectively. R_d is the dynamic resistance of the device at the bias point V_0 and $\beta = 1/k_bT$. Since the linewidth is proportional to the square of the dynamic resistance it is clear that the most favorable operating point for a junction biased to serve as a local oscillator is at the gap edge where R_d is smallest. Using device parameters that we have achieved for NbN/MgO/NbN

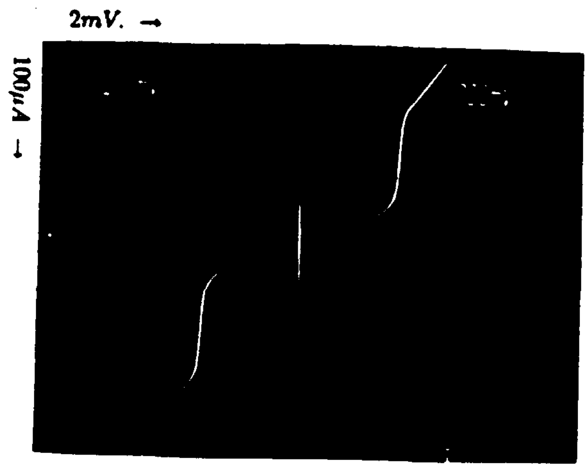

(a)

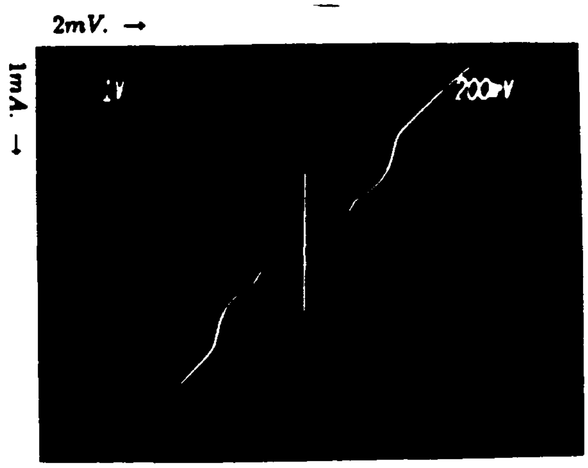

(b)

Figure 6. IV characteristics of several junctions; (a) $J_c = 5 \times 10^3 A/cm^2$ (b) $J_c = 4 \times 10^4 A/cm^2$.

tunnel junctions biased at the gap edge, $R_d = 2\Omega$, T = 10 K and $I_c = 200\mu A$ we find that

$$\left.\frac{\Delta\omega}{\omega}\right|_{\omega=2.3THz} = 4 \times 10^{-6} \qquad (6)$$

which should be suitable for mixing down to an IF frequency of 100 GHz. With a factor of 10 reduction of R_d at the gap edge, which is not an unreasonable goal the line width would be further reduced by a factor of 100. Such a reduction in R_d could probably be achieved through the fabrication of junctions with improved characteristics, or through the use of a stripline resonator or junction arrays.

In conclusion, we have investigated the feasibility of using high current density Josephson tunnel junctions as very high frequency local oscillators. Experiments with capacitively coupled junctions demonstrate that sufficient power can be coupled out of the junctions at frequencies in excess of 1 THz. We have developed an all refractory NbN/MgO/NbN tunnel junction process to raise both the LO power output and frequency, as well as the operating temperature of the device to the 10 K range. Future work will include raising the current density of these junctions as well as capacitively coupling them to a second junction to extend our measurements of LO power output to frequencies above 2 THz.

5. Acknowledgements

This work was sponsored by AF contract F19628-86-K-0034 with RADC, funded by SDIO/IST.

6. References

1. B. D. Hunt, R. A. Buhrman, IEEE Trans. Magn., Mag-19, 1155, 1983.

2. D. Rogovin and D. J. Scalapino, "Fluctuation Phenomena in Tunnel Junctions", Ann. Phys., vol. 86, 1, 1974.

NbN Josephson Tunnel Junctions for Terahertz Local Oscillators

R. P. Robertazzi, R. A. Buhrman

School of Applied and Engineering Physics, Cornell University Ithaca, New York 14853-2501

Rugged, high current density, NbN(C)/MgO/NbN(C) tunnel junctions have been fabricated and tested as voltage tunable Josephson junction terahertz oscillators. The emitted radiation from these junctions is detected on chip by a second junction which is capacitively coupled to the first. For oscillator junctions with a critical current density of $J_c \sim 4 \times 10^4 A/cm^2$ we find that the junction oscillates with a voltage amplitude of $\sim$ 1.5 mV. The detected RF voltage level remains essentially constant from 300 GHz. to above 1 THz. The oscillator junction is producing $0.5 \mu W$ of terahertz radiation of which, due to impedance mismatch, $.01 \mu W$ is coupled into the detector junction.

For some time there has been much interest in the application of Josephson junctions as high frequency, voltage tunable oscillators. Although the power available from a single device is somewhat limited the use of these devices in a coupled array configuration could significantly boost the available power [1]. A Josephson junction local oscillator incorporated into a millimeter and sub-millimeter wave receiver system, perhaps in conjunction with a superconductor - insulator - superconductor (SIS) mixer junction [2], is quite attractive. In order to maximize both the oscillation frequency and power output of such oscillators high current density tunnel junctions with large superconducting energy gaps must be employed. NbN tunnel junctions appear attractive for this application because of the large energy gap of NbN as well as its high transition temperature which would allow operation in closed cycle refrigerators. Thus questions are raised concerning the successful fabrication, cooling, and oscillation behavior of high current density NbN tunnel junctions. In this paper we report on a capacitively coupled Josephson oscillator - Josephson detector experiment that addresses these questions and that demonstrates that NbN junctions can be successfully employed as local oscillators at frequencies well above 1 Thz.

The schematic for the integrated thin film microstructure used in this experiment is shown in figure 1. It consists of two SIS devices coupled at RF frequencies but DC isolated so that each may be individually biased. One junction is a mesa type [3] formed with NbN(C) [4,5] base and counter electrodes and an MgO barrier. The second junction is an edge type [6] utilizing a Nb base electrode with a native oxide Nb_2O_5 barrier and Sn counter electrode. In normal operation the mesa junction is biased to serve as the local oscillator and the edge junction serves as a Josephson RF detector. A Nb-Sn detector junction was used in this experiment to permit the study of the response of a Josephson junction at frequencies well in excess of the gap sum frequency. Details of those particular observations as well as the complete fabrication process for the device will be reported elsewhere; here we focus on the performance of the NbN oscillator junction.

A typical current - voltage (IV) curve of a high current density generator is shown in figure 2a. The gap sum sum of the detector (1.8 mV) is somewhat reduced from full theoretical value (2 mV) because of impurities in the Nb film. The generator gap sum is reduced from 5 mV to 4 mV because the NbN(C) is off stoichiometry. The edge junction base electrode together with the common Au wiring forms a transmission line which is capacitively coupled to the generator. The typical generator operating frequency is 1 Thz. At this frequency the signal wavelength is l = 130 μm (correcting for the dielectric constant of Al_2O_3, $\epsilon_{Al_2O_3} = 5$ [7]), which is much longer than the 10μ length of line between the generator and detector. Consequently we may approximate the phase of the signal as being constant over the length of the coupling structure and use a simple AC circuit to model the device. The equivalent circuit is shown in figure 3. C_c represents the coupling capacitor, L_p and C_p the parasitic inductance and capacitance respectively associated with the coupling structure. For the dimensions shown in figure 1 we have C_c= 0.7 pf, L_p = .24 ph, and C_p = 0.05 pf. This means that at an oscillator frequency of 2 Thz., for oscillator impedances of $\sim 1\Omega$, detector impedances of $\sim 20\Omega$ or greater, the coupling efficiency $\eta = V_d/V_g$, where V_d is the amplitude of the oscillator signal across the detector and V_g is the amplitude of the oscillator signal at the generator approaches unity. For the device whose IV characteristics are shown, taking the normal state resistances of the junctions, $R_g = 1.9\Omega$, $R_d = 110\Omega$, and $\eta \sim 1$. Furthermore η remains close to unity even for frequencies down to 100 GHz., *which represents a range of over a factor of 20 in frequency over which the coupling efficiency is essentially unity.*

When DC biased, the generator will produce an oscillating voltage signal V_g at a frequency determined by the Josephson relation

$$f = 2eV_{bias}/h. \qquad (1)$$

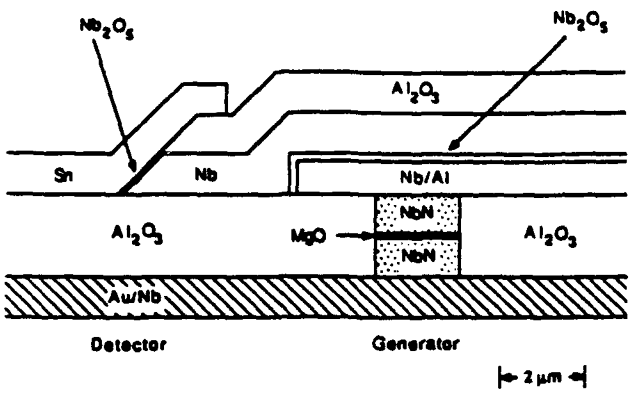

Figure 1: Integrated thin film microstructure used in the local oscillator experiments. The bimetallic layers are shown as single layers for clarity. Vertical scales are greatly exaggerated.

Here V_{bias} is the average voltage across the junction. V_g will be determined by the total capacitive loading of the generator. When the McCumber parameter β_c defined by [8]

$$\beta_c = (2e/\hbar)(I_cR)(RC) \qquad (2)$$

is less than unity the junction is not capacitively shunted and the maximum V_g obtainable is approximately I_cR_g, at least for $V_{bias} < 2\Delta$. Because the I_cR product is proportional to Δ, larger oscillator signal amplitudes, as well as higher frequencies, are possible with higher Δ materials. This is part of the motivation in the choice of NbN(C) for the generator base and counter electrodes. The capacitance in expression (2) is the total capacitance seen by the generator at the oscillation frequency which by design of the coupling structure is dominated by the junction capacitance. For a deposited MgO barrier 10 Å thick this capacitance is C = 0.3 pf assuming $\epsilon_{MgO} = 9.6$ [3]. This gives $\beta_c(gen) = 5.8$ so the generator is partially shunted and its IV characteristic is hysteretic.

When the generator is DC biased and if it emits radiation of sufficient power constant voltage Shapiro steps will be induced in the IV of the detector at integral multiples of V_{bias} [9]. Figure 2b shows the detector characteristic with the generator biased at 1.090 mV. The N = 1 and N = 2 steps are clearly visible, as well as the depression of the supercurrent (N = 0 step). The detector sees at RF frequencies a low impedance generator, consequently it is appropriate to model the detector as being driven by an RF voltage source. According to the voltage biased theory [10] the size of the Nth induced step is given by

$$\Delta I_N = I_c\left|J_N(\alpha)\right|. \qquad (3)$$

Here $\alpha = 2eV_d/hf = V_d/V_{bias}$, and $J_N(x)$ is the Bessel function of the first kind of order N. For the steps on the detector IV in figure 2b both the generator and detector

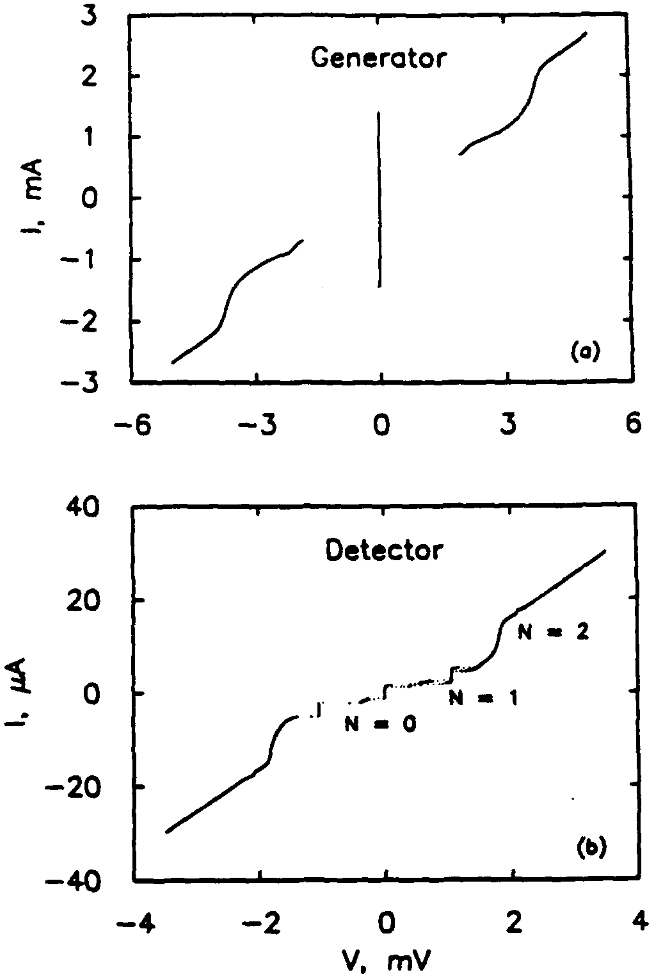

Figure 2: (a) IV characteristic of generator, $J_c = 3.5 \times 10^4 A/cm^2$, $R_n = 1.9\Omega$. (b) IV characteristic of detector, $J_c = 2.3 \times 10^3 A/cm^2$, $R_n = 110\Omega$ with generator biased at $V_{bias} = 1.090$ mV. The N = 1 and N = 2 Josephson steps are marked, as is the supercurrent (N = 0).

critical currents were suppressed by a magnetic field used to allow biasing the generator at this low frequency. The detected generated power is thus reduced. By taking the ratio of the current widths of the N = 0 and N = 1 steps and using equation (3) we may solve for α. This is more accurate than applying equation (3) directly since flux trapping makes the precise determination of I_c difficult.

Assuming a coupling efficiency of unity we find $V_g = 1.54$ mV, 58 % of the maximum value of 2.66 mV set by the I_cR product in the low β_c limit. While according to equation (2) to achieve the $\beta_c \sim 1$ limit a critical current density of $J_c = 3 \times 10^5 A/cm^2$ is required we find that with a hysteretic IV characteristic and a generator critical current density of $J_c = 3.5 \times 10^4 A/cm^2$ an RF power of 12 nW is being coupled into the 110Ω detector junction. This corresponds to a peak generator power of $V_g{}^2/2R_g = 0.6\ \mu W$ which is poorly coupled into the detector because of the large impedance mismatch (50 : 1) of the detector and generator. Thus the requirement on

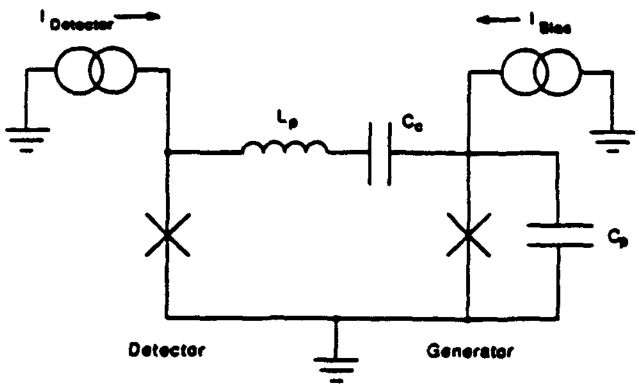

Figure 3: Equivalent circuit model of the double tunnel junction device.

J_c for a relatively high oscillator power level appears not to be severe.

In designing the biasing structure the self heating of the generator junction under bias and the local rise in temperature at the detector are important considerations. A measurement of the effectiveness of the biasing structure as a heat sink can be obtained by comparing the IV characteristic of the generator with the sample cell filled with He gas and then filled with He liquid to improve thermal contact to the bath. We have observed negligible changes in the gap sum voltage under these two conditions and conclude that self suppression effects of the generator are small at these current densities, assuming that, as is generally the case, heat transport away from the junction is substantially increased by the presence of liquid He. We may monitor the local temperature at the detector by measuring the Sn gap as a function of power dissipation of the generator. At a bath temperature of 1.5 K, we find that biasing the generator at 24 μW will raise the temperature of the detector 2.2 K, when only He exchange gas is present in the sample cell. With liquid He in the cell more than 5.5 times more power is required to produce the same temperature rise. When biased at the gap edge the generator dissipates 7.5 μW, so with liquid introduced into the cell adequate heat sinking should be obtainable with generator current densities well into the $10^5 A/cm^2$ range. Using an all NbN(C) detector junction would further reduce the effects of small temperature rises on detector performance.

We have measured the frequency dependence of the pair current response as the generator bias is tuned through the gap sum of the detector. At frequencies at and in excess of the gap-sum the expression (3) is no longer valid and the full high frequency theory which takes into account the frequency dependence of the pair current must be used [11]. Although our measurements are not in agreement with the high frequency theory above the gap sum they are consistent with previous measurements we have made on more closely coupled tunnel junctions [12]. Our results indicate that the generator is functioning at frequencies at least up to 1.4 THz. Experiments with a higher gap sum detector junction are now in progress to examine this high frequency limit in more detail.

In conclusion, we have fabricated a double tunnel junction device for experiments in using high current density Josephson tunnel junctions as high frequency local oscillators. The local oscillator is directly coupled to the detector by an RF capacitor, which allows highly efficient broad band coupling to be realized. We have succeeded in coupling at least 58% of the maximum LO voltage signal available into an SIS detector junction over a frequency range from 300 GHz. to 1.0 THz. The applications of a refinement of this device to heterodyne mixing are obvious. The incorporation of an all refractory detector junction into the device would raise the minimum operating temperature to 10 K, in the range of closed cycle He refrigerators.

This work was sponsored by Air Force contract F19628-86-K-0034 with RADC, funded by SDIO/IST and by the National Science Foundation through use of the facilities of the National Nanofabrication Facility and of the Cornell Materials Science Center.

References

[1] J. E. Sauvageau, A. K. Jain, J. E. Lukens, IEEE Trans. Magn., **Mag-23**, page 1048, 1987.

[2] P. L. Richards, IEEE Trans. Magn.,**Mag-23**, page 1247, 1987.

[3] Akira Shoji, Masahiro Aoyagi, Shin Kosaka, Fujitoshi Shinoki, Hisao Hayakawa, Appl. Phys. Lett., **46**, page 1098, 1985.

[4] S. A. Wolf, D. U. Gubser, T. L. Francavilla, E. F. Skelton, J. Vac. Sci. Technol., **18**, page 253, 1981.

[5] H. D. Hallen, Private Communication.

[6] A. W. Kleinsasser, R. A. Buhrman, Appl. Phys. Lett., **37**, page 841, 1980.

[7] B. W. Davis, Infrared Physics, **22**, page 91, 1982. Value of $\epsilon_{Al_2O_3}$ extrapolated from low frequency IR transmission data on sapphire.

[8] D. E. McCumber, J. Appl. Phys., **39**, page 3113, 1968.

[9] S. Shapiro, Phys. Rev. Lett., **11**, page 80, 1963.

[10] S. Shapiro, A. R. Janus, S. Holly, Rev. Mod. Phys., **36**, page 223, 1964.

[11] N. R. Werthamer, Phys. Rev., **147**, page 255, 1966.

[12] R. P. Robertazzi, B. D. Hunt, R. A. Buhrman, IEEE Trans. Magn., **Mag-23**, page 1271, 1987.

DISTRIBUTION LIST

RADC/EEAA ATTN: John P. Turtle Hanscom AFB MA 01731-5000	5
MR. ROBERT BUHRMAN CORNELL UNIVERSITY SCHOOL OF APPLIED AND ENG.PHYSICS CLARK HALL ITHACA NY 14853-2501	5
RADC/DOVL Technical Library Griffiss AFB NY 13441-5700	1
Administrator Defense Technical Info Center DTIC-FDAC Cameron Station Building 5 Alexandria VA 22304-6145	2
Strategic Defense Initiative Office Office of the Secretary of Defense Wash DC 20301-7100	2
Naval Warfare Assessment Center GIDEP Operations Center/Code 30G ATTN: E Richards Corona CA 91720	1
HQ SAC/SCPT OFFUTT AFB NE 68046	2
SM-ALC/MACEA ATTN: Danny McClure Bldg 237, MASOF McClellan AFB CA 95652	1
AFIT/LDEE Building 642, Area B Wright-Patterson AFB OH 45433-6583	1

WRDC/MTEL Wright-Patterson AFB OH 45433	1
AUL/LSE Bldg 1405 Maxwell AFB AL 36112-5564	1
HQ ATC/TTOI ATTN: Lt Col Killian Randolph AFB TX 78150-5001	1
AFLMC/LGY ATTN: Maj. Shaffer Building 205 Gunter AFS AL 36114-6693	1
Commanding Officer Naval Avionics Center Library D/765 Indianapolis IN 46219-2189	1
Cmdr Naval Weapons Center Technical Library/C3431 China Lake CA 93555-6001	1
Superintendent Code 1424 Naval Postgraduate School Monterey CA 93943-5000	1
CDR, U.S. Army Missile Command Redstone Scientific Info Center AMSMI-RD-CS-R/ILL Documents Redstone Arsenal AL 35898-5241	2
Los Alamos National Laboratory Report Library MS 5000 Los Alamos NM 87544	1

ESD/XRR
Hanscom AFB MA 01731-5000 1

SEI JPO 1
ATTN: Major Charles J. Ryan
Carnegie Mellon University
Pittsburgh PA 15213-3890

Director NSA/CSS 1
T5122/TDL
ATTN: D W Marjarum
Fort Meade MD 20755-6000

Director 1
NSA/CSS
W11 DEFSMAC
ATTN: Mr. Mark E. Clesh
Fort George G. Meade MD 20755-6000

DoD 1
R31
9800 Savage Road
Ft. Meade MD 20755-6000

DIRNSA 1
R509
9800 Savage Road
Ft Meade MD 20775

DOD Computer Center 1
C/TIC
9800 Savage Road
Fort George G. Meade MD 20755-6000

MISSION

OF

ROME LABORATORY

Rome Laboratory plans and executes an interdisciplinary program in research, development, test, and technology transition in support of Air Force Command, Control, Communications and Intelligence (C^3I) activities for all Air Force platforms. It also executes selected acquisition programs in several areas of expertise. Technical and engineering support within areas of competence is provided to ESD Program Offices (POs) and other ESD elements to perform effective acquisition of C^3I systems. In addition, Rome Laboratory's technology supports other AFSC Product Divisions, the Air Force user community, and other DOD and non-DOD agencies. Rome Laboratory maintains technical competence and research programs in areas including, but not limited to, communications, command and control, battle management, intelligence information processing, computational sciences and software producibility, wide area surveillance/sensors, signal processing, solid state sciences, photonics, electromagnetic technology, superconductivity, and electronic reliability/maintainability and testability.